Perfectly Matched Layers 1D

Semester Project

Laboratoire de simulation en mécanique des solides (LSMS)

Ecole Polytechnique Fédérale de Lausanne 2017-2018

September 2017 - February 2017

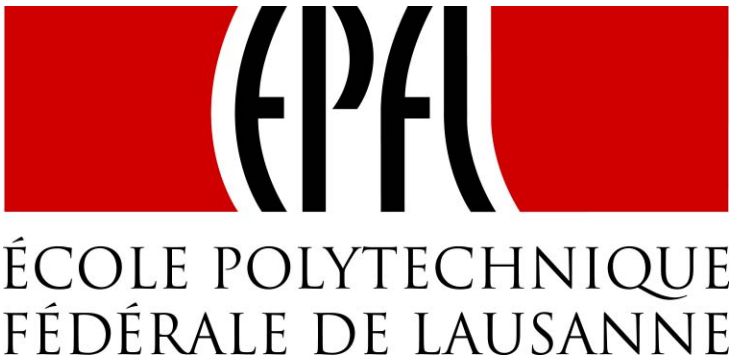

Student : Alexandre Poulain

Project supervisor : Michael Brun

Laboratory director : Jean-François Molinari

January 2018

Abstract

Absorbing boundary layers are widely employed to solve numerically wave propagation phenomena in infinite or unbounded domains. Several techniques exist to construct these boundaries such as Rayleigh damping in the absorbing layer or as presented in this report, perfectly matched layers (PML). Since the construction of these PMLs includes many aspects, this remains a challenge and several past researches lead for example in the case of the split-field PML for anisotropic problem to unstable solutions. We attend in this report to present a stable one dimensional PML based on the weak form of the equations of elastodynamics. First of all, the presentation of the construction of these PML will be detailed, including an extensive description of the equations governing this latter. The second part will be dedicated to the numerical results for test cases : a special attention will be dedicated to the reflection of the waves. We will shortly see that the PML is efficient to attenuate incident wave with less than 1 percent of the incident wave reflected in some extreme cases where the length of the PML and the coefficients of the attenuation function are reduced to their minimum. The last part will describe the proof of the stability : the stability of the numerical scheme will be proved first and the theoretical stability will be reviewed after that since stability of one doesn't lead to stability of the other.

Table des matières

Introduction

The study of wave propagation in unbounded media is an important topic for many research and engineering applications. The solution of the elastodynamic problem is interesting for the simulation of earthquake ground motion or for soil-structure problems where the reflection of the wave at the boundary needs to be eliminated. To address this problem, a common practice is to add a layer surrounding the domain of interest in order to absorb the wave propagating outward. Thus due to these boundaries the reflection is eliminated.

Different methods have been developed to simulate wave propagation in unbounded media : the infinite elements methods, originally developed by Ungless [28] and Bettess [25], which is close to the concept of finite elements but adds a new formulation including an infinite extent of the element region and shape functions. This method allows the approximation of the decaying laws governing the waves radiation process at infinity. The technique used here is to use finite element with their end nodes placed at infinity. The issues encountered with such technique is the same as the following method. The appropriate absorbing boundary conditions is a method involving specific conditions at the model boundaries to approximate the radiation condition for the elastic waves [4]. The definition of these boundaries using this method leads to non stable scheme and spurious reflections cannot be avoided. These conditions are also not useful for practical calculations since they involve complex system of equations. The two first methods presented here presents the same drawbacks in terms of computation and analysis. However in order to solve these problems other methods have been developed leading to more efficient schemes.
As presented in this report, another method is to define a new layer to the simulation : An absorbing layer. The Rayleigh Damping layers is based on a Rayleigh/Caughey damping formulation to express the damping matrix $[C]$ in the classic formulation of elastodynamic problems. This damping matrix in the Rayleigh formulation can be expressed as a combination of stiffness and mass matrix. This damping matrix for finite elements is often already available in existing Finite Element software which makes this method really practical to use. In [30], the efficiency of the method is given and shows a satisfactory behaviour of the method in terms of efficiency for the one and the two dimensional case.
Perfectly matched layers is another absorbing boundary layers method, that absorbs almost perfectly incident waves without any reflection from the truncation interface for all angles of incidence and frequencies. The wave entering into the PML decays with distance according to a user-defined decay function. The property of the non-reflection at the truncation interface is true in theory for the continuum case. Once a spatial discretization is used, numerical reflections are present but they can be attenuated using the parameters of the PML. These user-defined parameters can also increase the accuracy of the scheme used and even reduce the computational cost. Perfectly matched layers is a concept first introduced by Bérenger for the simulation of electromagnetic waves [19]. He used a split-field formulation and it arises from the use of complex-valued coordinate stretching in the electromagnetic wave equations [10]. The field-splitting formulation permits to avoid convolutional operations in the time domain when the resulting forms are inverted back into the frequency domain and it is based on the partition of the variables into two components : parallel and perpendicular to the truncation boundary. The drawback of this technique is that it alters the structure of the underlying differential equations and thus increases the number of unknowns. Another problem with Bérenger's split-field PML is that the problem is only weakly well-posed and thus prones to instability [2]. This led to the development of strongly well-posed unsplit formulation [1] but it turns out that these formulations also suffer from instability and need further manipulation of the equations to ensure it [3]. However, the PML have been adapted for other linear wave equations such as the Helmholtz equation (scalar wave equation) [27, 33, 17], linearised Euler equations [16] or for the wave propagation in poroelastic materials [36]. An extensive discussion of these different methods is beyond the scope of this report since we focus on elastodynamic problems.

Indeed, the concept of PML was first adapted to elastodynamic wave propagation problems by Hastings et al [18]. This formulation was obtained by taking the split-field formulation of Bérenger and directly applying it to the P- and S-wave potentials. This formulation was obtained in term of displacement potentials and yields to a velocity-stress finite-difference method. The proof of the absorptive property of the PML was developed by Chew and Liu [9] : they developed in the same time a new split-field formulation for isotropic media using complex-valued coordinate stretching to obtain the equations governing the PML. Following the same idea Liu [26] introduced a split-field PMLs for time-dependent elastic waves in cylindrical and spherical coordinates. Other split-field, time-domain PMLs for the velocity–stress formulation have been obtained and we refer to [37, 12, 8] for the details of these methods and the presentation of a finite-differences-time-domain (FDTD) implementation of them. Another split-field formulation was introduced by Komatitsch and Tromp [20] where the stress term is eliminated and the displacement is split into four components. This results in a third-order in time semi-discrete forms for the four displacement fields or can be expressed by a second-order system coupled with one first-order equation for one of the displacement field. The main drawback of their method is its complexity but it is the first displacement only formulation for elastodynamics.
As we have seen before split-field PML suffer from instability since they are weakly well-posed. Wang [35] introduced an unsplit formulation for finite-difference modeling of elastic wave propagation using convolution features (CPML). In contrast of the original formulation of CPML from the electromagnetic where they used complex-frequency-shifted stretching functions [32, 29], Wang used standard stretching functions for its PML implementation. In this report, we will develop an unsplit formulation using the finite element framework in the same spirit as Basu and Chopra. In [5], they introduced an unsplit-field PML for time-harmonic elastodynamics in 2D media. In [6], they developed the time-domain implementation of their PML and in [34], Basu extended its 2D formulation to 3D media using an explicit scheme.
Based on a decomposition of the elastodynamics equations as a first-order system, Cohen and Fauqueux [11] derived a split-field formulation where the strain tensor is split and they had to introduce independent stress variables to account for the split strain tensor components. This method was implemented using a mixed finite element approach and spectral elements. A different formulation was obtained by Festa and Vilotte [15] where they followed classic lines for reducing the second-order displacement-only elastodynamic problem to a first-order in time system. Instead of slitting the strain tensor, they used split-fields for both the velocity and stress components. In the framework of unsplit PML, Drossaert and Giannopoulos [14] described an alternative implementation based on recursive integration (RIPML). But this implementation presents less performance than the CPML for elastodynamics using the complex-frequency-shifted stretching functions[13]. Meza-Fajardo and Papageorgiou [24] discussed a novel PML approach. In the standard approach of PML the coordinate-stretching and associated decay functions are used along the direction normal to the PML interface. Meza-Fajardo and Papageorgiou introduced them along all coordinate directions resulting in a split-field, non-convolutional M-PML which shows superior performance compared to standard PML.
All this literature survey of the different formulation of the PML can be summarised in the following table borrowed from [21] :

Implementation	split-field	unsplit-field
FD	Chew and Liu [9]	Wang and Tang [35]
	Hastings et al. [18]	Drossaert and Giannopoulos [14, 13]
	Liu[26]	Komatitsch and Martin [20]
	Collino and Tsogka [12]	
FE/SE	Bécache et al. [8]	Basu and Chopra [5]
	Komatitsch and Tromp [20]	Basu [6]
	Cohen and Fauqueux [11]	
	Festa and Vilotte [15]	
	Meza-Fajardo and Papageorgiou [24]	

TABLE 1 – PML implementations in time-domain elastodynamics

The stability of the PML have been studied for mostly isotropic cases but Collino and Tsogka [12] showed that the split-field standard PML is adequate in the case of anisotropic conditions. Also Bécache [7] studied the stability of the PML and the effect of anisotropy : She showed that the standard PML is stable for isotropic cases and conditionally unstable for anisotropic applications. Bécache also proposed necessary conditions for stability in the form of inequalities choice of the stretching function.
In the light of these previous works we will attend in this report to describe the formulation of a one dimensional unsplit-field displacement-based PML. Its implementation will be done in the framework of finite elements. First of all we will describe in details the construction of the equations of the PML and also its formulation in the context of finite elements. After this theoretical description, the numerical results obtained on test case involving a Ricker wave will be presented. In the last part, we will discuss the stability of the PML : Theoretical and numerical stability will be presented as well as the proof of the well-posedness of the problem.

1 Description

In this part we will describe the construction of the one dimensional PML from elastodynamics wave equations to the finite elements formulation.

1.1 Elastic medium

In the following of this report we will consider a one dimensional homogeneous isotropic elastic continuum. In such medium the displacement $u(x,t)$ is governed by the following equations :

$$\begin{aligned} \frac{\partial \sigma}{\partial x} &= \rho \ddot{u} \\ \sigma &= E\epsilon \\ \epsilon &= \frac{\partial u}{\partial x} \end{aligned} \tag{1}$$

In the equations of 1 and in the following of this report we will omit the dependence on x and t since, without any indications, is obvious. In fact the displacement u, the stress σ, the strain ϵ and the acceleration $\ddot{u}$ are scalar functions. ρ is the density and E is the young modulus of the medium.

1.2 Strong form of the PML in the frequency domain

As in the work of Basu and Chopra [5] we first begin by introducing the complex-valued coordinate stretching functions λ which is a non-zeros function everywhere. The idea is to replace the real coordinates x by the complex ones $x \to \tilde{x} : \mathbb{R} \to \mathbb{C}$. This function represents a mapping of the real spatial coordinates onto the complex space. Let us also introduce the attenuation functions f^p and f^e : an explicit formulation of this functions will be described later in this report. f^p is used to attenuate propagating waves and f^e in other hand serves to attenuate evanescent waves. Both of these real-valued positive functions vanish at the interface between the physical medium and the PML so that the PML matches perfectly the physical domain. The complex coordinates are defined by :

$$\begin{aligned} \tilde{x} &= \int_{s=0}^{x} \lambda(s,\omega) ds \\ &= \int_{s=0}^{x} \left[1 + f^e(s) + \frac{c_s}{i\omega L_p} f^p(s) \right] ds \end{aligned} \tag{2}$$

And the derivative with respect to x by :

$$\frac{\partial \tilde{x}}{\partial x} = 1 + f^e(x) + \frac{c_s}{i\omega L_p} f^p(x) = \lambda(x) = 1 + f^e(x) - \frac{i c_s}{\omega L_p} f^p(x) \tag{3}$$

In the equations 2 and 3 c_s stands for the celerity of the S-waves and L_p is the length of the PML. The functions of attenuation have the following the expressions :

$$f^p(x) = \alpha_p \left(\frac{x - x_0}{L_p} \right)^m \tag{4}$$

$$f^e(x) = \alpha_e \left(\frac{x - x_0}{L_p} \right)^m \tag{5}$$

In the equations 4 and 5, $\alpha_p > 0$ and $\alpha_e > 0$ respectively are the coefficients of attenuation for propagating and evanescent waves. Using these complex coordinates we can express the governing equations of motion in the frequency domain :

$$\frac{1}{\lambda(x)}\frac{\partial \overline{\sigma}}{\partial x} = -\rho\omega^2\overline{u} \tag{6}$$

In equation 6, ρ is the density of the PML, σ is the stress tensor and $u(x,t)$ is the position. The line over the elements define that they are defined in the frequency domain. In the following of this report we will omit the dependence on x. We can express the derivative of the stress tensor :

$$\begin{aligned}\frac{\partial \overline{\sigma}}{\partial x} &= \rho(i\omega)^2\overline{u}\left[(1+f^e(x)) + \frac{c_s}{i\omega L_p}f^p(x)\right] \\ &= \rho(i\omega)^2(1+f^e(x))\overline{u} + \frac{c_s}{L_p}(i\omega)f^p(x)\overline{u}\end{aligned} \tag{7}$$

Using the inverse Fourier transform, we obtain the equation of motion in the time domain :

$$\frac{\partial \sigma}{\partial x} = (1+f^e(x))\rho\ddot{u} + \frac{\rho c_s}{L_p}f^p(x)\dot{u} \tag{8}$$

Since we place ourselves in the context of linear elastic we have the constitutive relationship :

$$\sigma = E\epsilon \tag{9}$$

with E the Young modulus of the PML. Let us now introduce the strain-displacement relationship in the frequency domain :

$$\overline{\epsilon} = \frac{1}{2}\left(\frac{\partial \overline{u}}{\partial x}\frac{\partial x}{\partial \tilde{x}} + \frac{\partial \overline{u}}{\partial x}\frac{\partial x}{\partial \tilde{x}}\right) = \frac{\partial \overline{u}}{\partial x}\frac{\partial x}{\partial \tilde{x}} = \frac{\partial \overline{u}}{\partial x}\frac{1}{\lambda} \tag{10}$$

Using this equation and the expression of the stretching function 3 we can define the following equivalence :

$$\lambda\overline{\epsilon} = \frac{\partial \overline{u}}{\partial x} \iff \left(1 + f^e(x) + \frac{c_s}{i\omega L_p}f^p(x)\right)\overline{\epsilon} = \frac{\partial \overline{u}}{\partial x} \tag{11}$$

Again using the inverse Fourier transform, we can recast the previous equation 11 in the time domain :

$$(1+f^e(x))\epsilon + \frac{c_s}{L_p}f^p(x)H = \frac{\partial u}{\partial x} \tag{12}$$

with $H = \int_0^t \epsilon(x,s)ds$.
The strong form of the PML in the time domain is obtained using the equations 12, 8 and 9. To summarize the problem obtained so far we can recall these equation into the following problem :

$$\begin{aligned}\frac{\partial \sigma}{\partial x} &= (1+f^e(x))\rho\ddot{u} + \frac{\rho c_s}{L_p}f^p(x)\dot{u} \\ \sigma &= E\epsilon \\ \frac{\partial u}{\partial x} &= (1+f^e(x))\epsilon + \frac{c_s}{L_p}f^p(x)H\end{aligned} \tag{13}$$

1.3 Weak form of the PML and finite elements formulation

Following the work of Basu and Chopra [5], we will use a displacement-based space discretization in the framework of standard finite elements. Thus let v be the compactly supported test function vanishing at the boundaries and belonging to an appropriate space V. The weak formulation of the PML is obtained by multiplying the left and right sides of 8 by v and then integrating the all equation over the computational domain Ω.

$$\int_\Omega \frac{\partial \sigma}{\partial x} v \mathrm{d}\Omega = \int_\Omega (1 + f^e(x)) \rho \ddot{u} v \mathrm{d}\Omega + \int_\Omega \frac{\rho c_s}{L_p} f^p(x) \dot{u} v \mathrm{d}\Omega \tag{14}$$

Let us focus on the left hand side of the equation 14, integration by parts yields to the following expression :

$$LHS = -\int_\Omega \sigma \frac{\partial v}{\partial x} \mathrm{d}\Omega + \int_{\partial\Omega} v \cdot \sigma n \mathrm{d}S \tag{15}$$

The test have been chosen such that it vanishes at the boundary of the computational domain. Therefore the rightmost term of the equation 15 is equal to $\int_{\partial\Omega_p} v \cdot \sigma n \mathrm{d}S = 0$. Using the finite elements method, we can define the basis functions as :

$$N_i(x_j) \begin{cases} 1, & \text{if } x_j = x_i \\ 0, & \text{Otherwise} \end{cases} \tag{16}$$

Therefore for one bar element composed of two nodes $[-1, 1]$ we can define the following basis functions :

$$\begin{cases} N_1(x) = \frac{1}{2}(1 - x) \\ N_2(x) = \frac{1}{2}(1 + x) \end{cases} \tag{17}$$

Using this basis functions for each element the components of the problem can be decomposed as a linear combination of this two functions.

$$u_e(x) = \sum_{i=1}^{2} u_i(t) N_i(x) \tag{18}$$

with $x \in [-1, 1]$, $u_i(t)$ a time dependent coefficient. As we can see we get rid of the spatial dependence for the coefficient u_i and we can move it out of the integrals. Thus for each element Ω_e the weak form of the equation of motion in the PML can be rewrite as :

$$\{v_e\}^T \int_{\Omega_e} (1 + f^e(x)) \, \rho \, [N]^T [N] \, \mathrm{d}\Omega_e \, \{\ddot{u}_e\} + \{v_e\}^T \int_{\Omega_e} \frac{\rho c_s}{L_p} [N]^T [N] \, \mathrm{d}\Omega_e \, \{\dot{u}_e\} + \int_{\Omega_e} \left(\frac{\partial v}{\partial x} \sigma \right) \mathrm{d}\Omega_e = 0 \tag{19}$$

With $\{v_e\} = \begin{bmatrix} v_1 \\ v_2 \end{bmatrix}$ with v_1 and v_2 being respectively the value of the coefficient at the node 1 and 2. To solve the problem of the partial derivative with respect to x, we need to introduce the simple first order approximation operator $[B] = \frac{1}{L_e} \begin{bmatrix} 1 & -1 \end{bmatrix}$ with L_e the length of an element.

$$\frac{\partial v_e}{\partial x} = [B] \{v_e\} \tag{20}$$

Thus the right most term can be rewrite as :

$$\int_{\Omega_e} \left(\frac{\partial v}{\partial x} \sigma \right) \mathrm{d}\Omega_e = \{v_e\}^T \int_{\Omega_e} [B]^T \sigma \mathrm{d}\Omega_e \tag{21}$$

Since we consider an one dimensional bar element, the integral over the element can be re-expressed as :

$$\mathrm{d}\Omega_e = S \frac{L_e}{2} \mathrm{d}\xi \tag{22}$$

With S the section of the bar element. This leads us to the following formulation :

$$M_e \{\ddot{u}_e\} + C_e \{\dot{u}_e\} + P_{e,int} = 0 \tag{23}$$

With

$$M_e = \int_{\xi=-1}^{1} (1 + f^e(\xi))\rho [N]^T [N] S \frac{L_e}{2} \mathrm{d}\xi \tag{24}$$

$$C_e = \int_{\xi=-1}^{1} \frac{\rho c_s}{L_p} f^p(\xi) [N]^T [N] S \frac{L_e}{2} \mathrm{d}\xi \tag{25}$$

And

$$P_{e,int} = \int_{\xi=-1}^{1} [B]^T \sigma S \frac{L_e}{2} \mathrm{d}\xi \tag{26}$$

We can clearly recognise here the same formulation as the standard elastodynamic problem. In fact if we think about the formulation over the all computational domain, we retrieve the following formulation :

$$M \{\ddot{u}\} + C \{\dot{u}\} + P_{int} = 0 \tag{27}$$

Where M, the mass matrix, is defined per blocks of shape 2×2 on the diagonal using the equation 24 and we can obtain the same for C, the damping matrix, using the formula 25.
The only problem remaining in this formulation is the stress in the expression of the internal forces P_{int}. In fact we will give an explicit formulation of this latter concurrently with the description of the temporal discretization and the presentation of the temporal integration method used.

1.4 Temporal discretization

We will consider a simple time discretization $t = nh = t^n$ with h the step of the temporal discretization and n the index. If we consider the time step $n + 1$ and go back to the equation 12 we can write :

$$\begin{aligned} \frac{\partial u^{n+1}}{\partial x} &= (1 + f^e(x))\epsilon^{n+1} + \frac{c_s}{L_p} H^{n+1} \\ &= (1 + f^e(x))\epsilon^{n+1} + \frac{c_s}{L_p} \left(H^n + h\epsilon^{n+1}\right) \end{aligned} \tag{28}$$

This expression is obtained by the temporal discretization and its effect on $H = \int_0^t \epsilon(x, s)ds$ turning this expression into $H^{n+1} = k \sum_{i=0}^{n+1} \epsilon(x, t^i)$. We can change the equation 28 by factorising by ϵ^{n+1} :

$$\left[(1 + f^e(x)) + \frac{hc_s}{L_p} f^p(x)\right] \epsilon^{n+1} = \frac{\partial u^{n+1}}{\partial x} - \frac{c_s f^p(x)}{L_p} H^n \tag{29}$$

Using this equation and the first order approximation of the spatial derivative we can express the stress using Hooke's law 9 :

$$\begin{aligned} \sigma^{n+1} &= E\epsilon^{n+1} \\ &= \frac{E}{\alpha(x)} [B] \left\{u_e^{n+1}\right\} - \frac{Ec_s f^p(x)}{\alpha(x) L_p} H^n \end{aligned} \tag{30}$$

With $\alpha(x) = \left[(1 + f^e(x)) + \frac{hc_s}{L_p} f^p(x)\right]$. The expression of the internal forces for an element is given by the equation 26, expressing this equation at time $n + 1$ and using the expression of the stress 30 we obtain :

$$\begin{aligned} P_{e,int}^{n+1} &= \int_{\xi=-1}^{1} [B]^T \sigma^{n+1} S \frac{L_e}{2} \mathrm{d}\xi \\ &= \left(\int_{\xi=-1}^{1} \frac{E}{\alpha(\xi)} [B]^T [B] S \frac{L_e}{2} \mathrm{d}\xi\right) \left\{u_e^{n+1}\right\} - \left(\int_{\xi=-1}^{1} [B]^T \frac{c_s}{L_p} \frac{f^p(\xi)}{\alpha(\xi)} E H^n S \frac{L_e}{2} \mathrm{d}\xi\right) \end{aligned} \tag{31}$$

Thus the stiffness matrix K can be defined per bloc as the mass and damping matrices. The blocs have the following form :

$$K_e = \int_{\xi=-1}^{1} \frac{E}{\alpha(\xi)} [B]^T [B] S \frac{L_e}{2} \mathrm{d}\xi \tag{32}$$

Therefore for each element we obtain the following equation :

$$[M_e] \{\ddot{u}_e^n\} + [C_e] \{\dot{u}_e^n\} + [K_e] \{u_e^n\} = \int_{\xi=-1}^{1} [B]^T \frac{c_s}{L_p} \frac{f^p(\xi)}{\alpha(\xi)} E H^n S \frac{L_e}{2} \mathrm{d}\xi \tag{33}$$

The right hand side term is the internal forces at time n : $P_{e,int}^n$. Therefore we obtain for the all computational domain the following relation :

$$[M] \{\ddot{u}^n\} + [C] \{\dot{u}^n\} + [K] \{u^n\} = P_{int}^n \tag{34}$$

We can observe that our unknowns are the displacement u, the velocity $\dot{u}$, the acceleration $\ddot{u}$ and the internal forces P_{int}. An important remark is the number of unknowns of our formulation of the unsplit-field PML is lesser than for split-field standard PML.
In order to resolve the temporal integration, we will employ a standard Newmark-β scheme and the integrals over the each element will be evaluated using Gauss quadrature. In our case we used two points of quadrature in order to obtain an approximate value of the integral. For each element we have the two quadrature points $\xi_1 = -\frac{1}{\sqrt{3}}$ and $\xi_2 = \frac{1}{\sqrt{3}}$ with their associated weights $w_1 = w_2 = 1$. Thus the integrals over the elements can be expressed as a sum of the interior of the integral evaluated at the quadrature points.

1.5 Algorithm

In order to give an overview of the algorithm, let us present the Newmark-β scheme used for the PML. We will consider the case of a one dimensional bar composed at the left with the physical medium and at the right the PML.

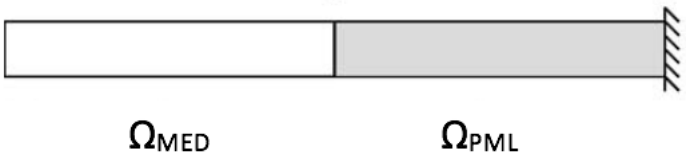

FIGURE 1 – Scheme of the 2 media : on the left physical medium and on the right the PML

We will impose at the extremity of the bar a force in order to create a wave. The other extremity corresponding to the end of the PML will be fixed. The algorithm will go through the following steps :

2 Methods and results

With the implementation of the PML and using the algorithm **??**, we can now proceed to the test of the one dimensional PML. To evaluate the performance, we will focus on the reflection of the wave from the interface and the wave coming back from the PML. The other parameter to be evaluate will be the computational cost in term of time. In fact the objective of such analysis is to find the best compromise between accuracy, minimising the reflection wave and the computational. Therefore we will be able to highlight the parameters to have the best result possible.

2.1 Inputs and parameters

In order to test the PML, we choose to place ourselves in the context of the problem described by the figure 1. A summary of the parameters used for the simulation can be found in the following table.

L_m	50
L_p	20
L_e	1
S	1
c_s	50
ρ	1700
E	$10e^5$
h	$0.8h_{CFL}$
T	500

TABLE 2 – Parameters for the PML and the medium

In the table 2, T stands for the end time. The time step h must be chosen carefully. This parameter is very important since we seek a balance between computational cost and accuracy. Of course increasing this parameter leads to a lower computational cost but also to a smaller accuracy. Another property determined by this parameter is also the stability of the numerical scheme. The method implemented in our case uses a GC coupled interface in order to be able to perform an explicit scheme on the medium while conserving an implicit one on the PML. Since explicit Newmark scheme is conditionally stable we need to ensure that the time step is smaller than the critical time step determine by the formula :

$$h_{CFL} = \frac{L_e}{\sqrt{\frac{E}{\rho}}} \tag{35}$$

A simple numerical application gives us in our case $h_{CFL} = 0.0412$. We ensured that the time step is below this critical time step. The parameters for the Newmark-β scheme are $\gamma = 0.5$ and $\beta = 0.25$. The last parameters to define are the ones for the attenuation functions. The order of the polynomials will be $m = 2$. The coefficients for the attenuation function for propagating wave is the most important to define due to its importance for the damping of the wave. If we assume that $\frac{c_s}{L_p} = 1$, the coefficient for this function and in the case of a propagating P-wave in a one dimensional medium can be expressed by the following formula [22] :

$$\alpha_p = \frac{(m+1)v_p}{2L_p} log\left(\frac{1}{R}\right) \tag{36}$$

where v_p is the velocity of the P-waves and R is the reflection coefficient from the outer PML boundary. This coefficient shows the amplitude reduction of the P wave entering into the PML. This parameter has to

be taken into account when we will evaluate the performance of the method. The value for the parameters in the expression of the coefficient α_p has, in our example, the following values :

v_p	76.7
R	10^{-3}
α_e	1

TABLE 3 – Parameters for the attenuation functions

As shown in the table 3, the coefficient of attenuation for evanescent wave is simply 0. Since this function does not have a large impact on the damping of the wave entering the PML : $f^e(x) = 0 \forall x$.

2.2 Ricker wave

In this numerical simulation, we will analyse the behavior of the PML against the propagation of non harmonic waves. A Ricker wave will be imposed at the free end of the physical medium in the form of a force. This external force has the following formula :

$$F_{ext} = A\left(2\pi^2\frac{(t-t_s)^2}{t_p^2} - 1\right) exp\left(-\pi^2\frac{(t-t_s)^2}{t_p^2}\right) \tag{37}$$

The Ricker wave is defined by 3 parameters : The fundamental period t_p, the time shift t_s and the amplitude A. These parameters take the values :

t_p	0.5s
t_s	1s
A	1

TABLE 4 – Values for the parameters of the Ricker Wave

Using this parameters the Ricker wave in the time domain has the following shape :

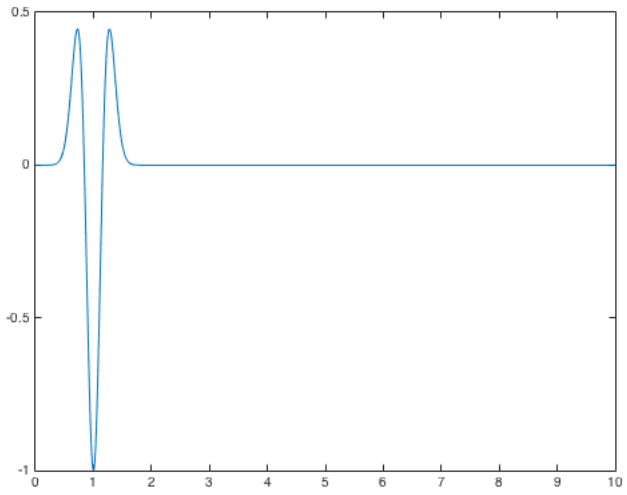

FIGURE 2 – Ricker wave in the time domain

2.3 Results

The measurement of the displacement and the velocity at the center of the physical medium gives a good insight of the propagation of the wave and of its possible reflection. Using the above parameters for the medium, the PML and the input wave, the following graphs are obtained :

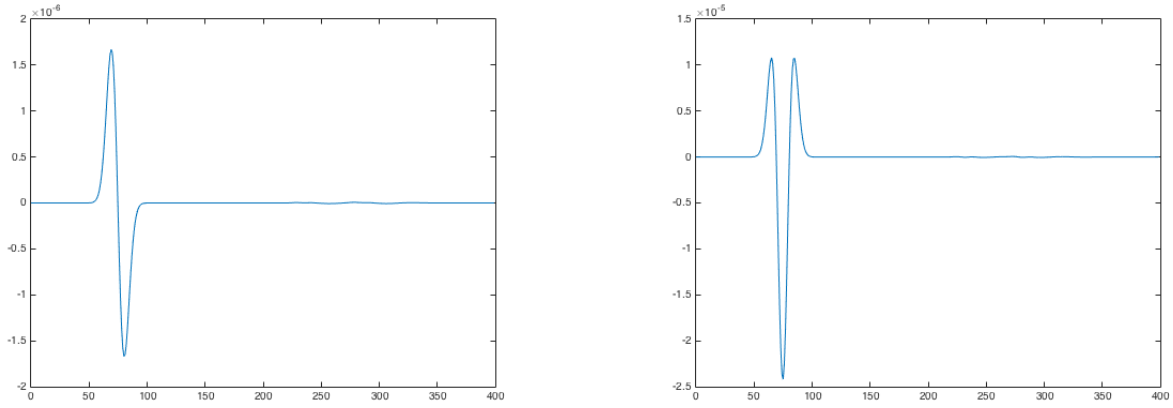

FIGURE 3 – Longitudinal displacement (right) and the velocity (left) at $x = 25m$ as a function of time

The figure 3 shows the displacement and the velocity through the time at the node placed at $x = 25m$. Looking at the figures 3 we can see that the PML reduced drastically the reflection of the incident wave at the interface. Therefore the PML seems accurate since we can barely see the reflection of the wave at the interface.

2.3.1 Reflection of the wave

In this part, we will focus on the reflection of the wave in function of different parameters. To be more precise, we will separate the reflection of the wake into two kinds : the reflection due to the interface and the reflected wave bouncing at the extremity of the PML and coming back into the medium. This study will focus on the effect of the parameters for the PML such as the length L_p and the attenuation coefficient α_p. The length of the elements L_e will also be tested and the last parameter tested will be the time step k.
First of all let us focus on the effect of the attenuation coefficient α_p.

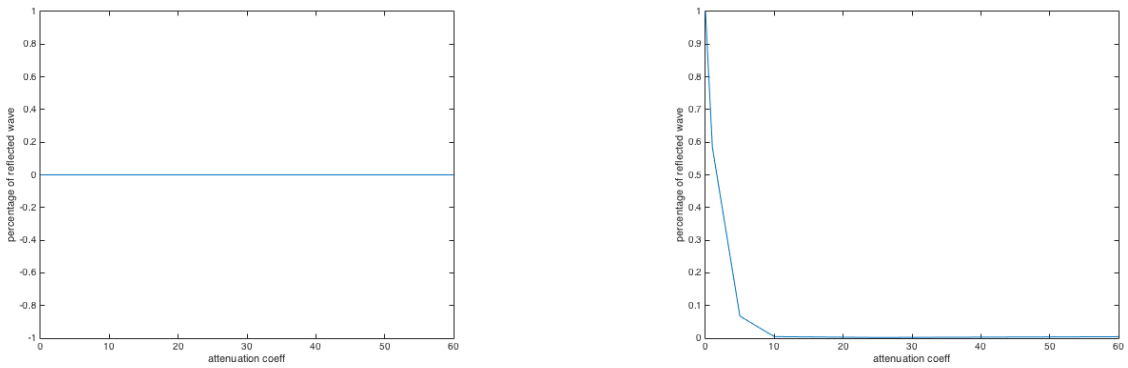

FIGURE 4 – Percentage of reflected wave due to the interface (left) and coming back from the extremity of PML (right) in function of α_p

As shown on the figure 4, the attenuation coefficient has no effect on the reflection of the wave at the interface : there is exactly no reflection due to the interface. The wave is damped in the PML in function of this coefficient as shown on the right figure. Indeed if $\alpha_p = 0$ There is no damping of the wave whereas if $\alpha_p = 10$ the wave is totally attenuated by the PML.
Let us now investigate the effect of the length of the PML. Since it has any effects on the interface we will focus only on the percentage of the wave coming back from the absorbing layer.

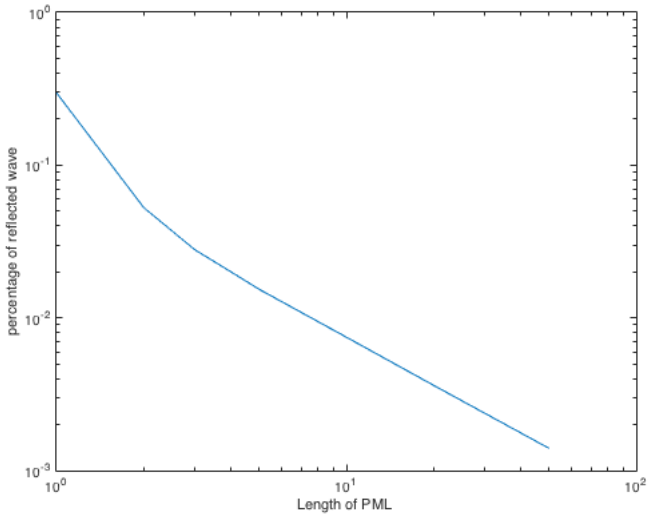

FIGURE 5 – Percentage of reflected wave in function of L_p

As we can observe on the figure 5, the percentage of the wave reflected at the fixed extremity of the PML and coming back in the physical medium decreases when the length of the PML increases.
Let us now focus on the length of the element L_e for 20 elements in the PML. Since the length of the PML and its coefficients of attenuation permits the complete attenuation of the incident wave, we will focus only on the reflection due to the interface.

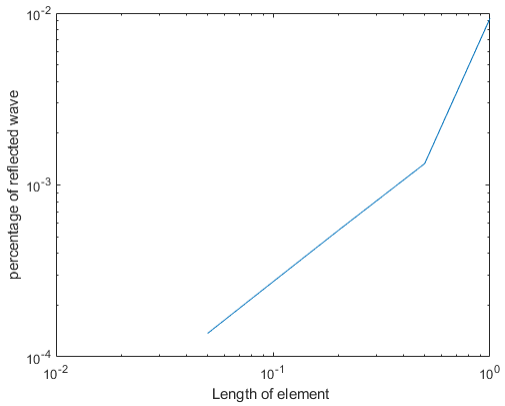

FIGURE 6 – Percentage of reflected wave at the interface in function of L_e

As we can see on the figure 6, the slope of the percentage of the reflected wave can be evaluated at L_e^1.

3 Stability

After evaluating numerically the overall efficiency of the method for the one dimensional case, the theoretical and numerical stability will be studied. In fact, the theoretical stability does not lead to the stability of the numerical scheme. Therefore, both stabilities will be studied separately

3.1 Theoretical stability

3.1.1 Well-posedness

The definition of the well-posedness is that a problem is said to be well-posed if it has a solution, that should be unique and should depend continuously on the data of the problem. This last requirement states that perturbations such as errors in measurement should not affect the solution in a too large proportion.

3.2 Stability of the numerical method

In order to prove the stability of the temporal scheme, we can recall the following result concerning integration methods [23] : An integration scheme is said to be stable if there exists an integration step $h_0 > 0$ so that for any $h \in [0, h_0]$, a finite variation of the state vector at time t^n induces only a non-increasing variation of the state vector q^{n+1} calculated at a subsequent instant t^{n+1}.
In our case we will study the stability of the scheme with the temporal discretization presented in part 1. This reduces to the analysis of the stability properties of the Newmark-β scheme used in the algorithm **??** for the PML uniquely. We will focus our attention of the stability of the temporal scheme applied on only one element. We can prove the stability on one element the result extends to the other element [31]. First of all we need to go back to the equations of motion and define the state vector : $Q^n = [\dot{u}^n, u^n, H^n]^T$. The objective is to define the matrices A and B such that :

$$A(h)Q^{n+1} + B(h)Q^n = 0 \tag{38}$$

which is in fact the matrix form of the equations of motion. Since each component of the state vector have the size 2×1, the matrices A and B are 6×6. This formulation comes from the fact that the we used have only one bar element composed of two points. Let us first recall the equation of motion at time t^n and t^{n+1} :

$$M\ddot{u}^n = -C\dot{u}^n - Ku^n + p_{int}^n \tag{39}$$

$$M\ddot{u}^{n+1} = -C\dot{u}^{n+1} - Ku^{n+1} + p_{int}^{n+1} \tag{40}$$

Using the recurrence relationship described in the algorithm **??** from the Newmark scheme, we obtain :

$$M\dot{u}^{n+1} = M\dot{u}^n + h(1-\gamma)\left[-C\dot{u}^n - Ku^n + p_{int}^n\right] + \gamma h\left[-C\dot{u}^{n+1} - Ku^{n+1} + p_{int}^{n+1}\right] \tag{41}$$

$$Mu^{n+1} = Mu^n + hM\dot{u}^n + h^2(\frac{1}{2} - \beta)\left[-C\dot{u}^n - Ku^n + p_{int}^n\right] + \beta h^2\left[-C\dot{u}^{n+1} - Ku^{n+1} + p_{int}^{n+1}\right] \tag{42}$$

With β and γ the parameters of the Newmark scheme. We also have a recurrence relation for H^{n+1}.

$$H^{n+1} = H^n + h\epsilon^{n+1} \tag{43}$$

With ϵ^{n+1} the strain at time t^{n+1} which can be expressed in function of u^{n+1} and H^n. The following formulation is element wise, since we consider the stability on only one element this formulation suffices :

$$\epsilon^{n+1^e} = \frac{[B]\{u^{n+1^e}\} - \frac{c_s}{L_p} f_x^p H^n}{\alpha} \tag{44}$$

with $\alpha = (1 + f_x^e) + \frac{c_s}{L_p} f_x^p$.
Using the equations 41, 42 and 43, we seek the definition of the matrix form 38. We will define the matrices per blocs of size 2×2. In the following development the mass M, damping C and stiffness K matrices are using the formulas 24, 25 and 32 for one element.
First of all, let us multiply by the left 41 and 42 by M^{-1} and put all the terms to the left side :

$$\dot{u}^{n+1}\left[I + \gamma h M^{-1}C\right] + u^{n+1}\left[\gamma h M^{-1}K\right] - \gamma h M^{-1} p_{int}^{n+1} + \dot{u}^n\left[-I + h(1-\gamma)M^{-1}C\right] + u^n\left[h(1-\gamma)M^{-1}K\right] - h(1-\gamma)M^{-1}p_{int}^n = 0 \quad (45)$$

$$\dot{u}^{n+1}\left[\beta h^2 M^{-1}C\right] + u^{n+1}\left[I + \beta h^2 M^{-1}K\right] - \beta h^2 M^{-1} p_{int}^{n+1} + \dot{u}^n\left[-hI + h^2(\frac{1}{2} - \beta)M^{-1}C\right] + u^n\left[-I + h^2(\frac{1}{2} - \beta)M^{-1}K\right] - h^2(\frac{1}{2} - \beta)M^{-1}p_{int}^n = 0 \quad (46)$$

The only problem remaining before constructing the matrices $A(h)$ and $B(h)$ is how to handle the term of the internal forces p_{int}. Let us recall its expression first :

$$p_{int}^n = \int_{-1}^{1} [B]^T \frac{c_s}{L_p} \frac{f^p(\xi)}{\alpha(\xi)} H^n S \frac{L_e}{2} d\xi \quad (47)$$

Since we assumed that f^p and f^e are constant and using the quadrature to evaluate the integral with two Gauss points with weights $w = 1$ we obtain

$$p_{int}^n = \frac{c_s}{L_p} ES \begin{bmatrix} \frac{2}{L_e} \\ \frac{-2}{L_e} \end{bmatrix} \begin{bmatrix} 1 \times \frac{H_{n,k=1} f_{k=1}^p}{\alpha_{k=1}} & 1 \times \frac{H_{n,k=2} f_{k=2}^p}{\alpha_{k=2}} \end{bmatrix} = \frac{c_s}{L_p} ES \frac{f^p}{\alpha} \begin{bmatrix} 1 & 1 \\ -1 & -1 \end{bmatrix} \begin{bmatrix} H_{n,k=1} \\ H_{n,k=2} \end{bmatrix} \quad (48)$$

where $k = 1$ corresponds to the first Gauss point and $k = 2$ to the second. We also have :

$$A_p = \frac{c_s ES}{L_p} \frac{f_x^p}{\alpha} \begin{bmatrix} 1 & 1 \\ -1 & -1 \end{bmatrix} \quad (49)$$

For the last row of the matrices we need to focus on the equation :

$$H^{n+1} = H^n + h\epsilon^{n+1} \quad (50)$$

with ϵ^{n+1} given by the equation 44 such that we obtain :

$$H^{n+1} + H^n\left[-I + h\frac{c_s}{L_p}\frac{f_x^p}{\alpha}\right] - \frac{h}{\alpha}\left[\overline{B}\right] u^{n+1} \quad (51)$$

$$A(h) = \begin{bmatrix} I + \gamma h M^{-1}C & \gamma h M^{-1}K & -\gamma h M^{-1}A_p \\ \beta h^2 M^{-1}C & I + \beta h^2 M^{-1}K & -\beta h^2 M^{-1}A_p \\ 0 & -\frac{h}{\alpha}\overline{B} & I \end{bmatrix} \quad (52)$$

where

$$\overline{B} = \frac{1}{L_e}\begin{bmatrix} -1 & 1 \\ -1 & 1 \end{bmatrix} \quad (53)$$

We expressed in 52 all the terms depending on time t^{n+1}, let us now express the remaining terms depending on time t^n :

$$B(h) = \begin{bmatrix} -I + (1-\gamma)hM^{-1}C & (1-\gamma)hM^{-1}K & -(1-\gamma)hM^{-1}A_p \\ -hI + (\frac{1}{2}-\beta)h^2M^{-1}C & -I + (\frac{1}{2}-\beta)h^2M^{-1}K & -(\frac{1}{2}-\beta)h^2M^{-1}A_p \\ 0 & 0 & -I + \frac{c_s}{L_p}\frac{f_x^p}{\alpha}I \end{bmatrix} \tag{54}$$

Using the equation 52 and 54, we can define the amplification matrix associated with the integration operator $H(h) = A(h)^{-1}B(h)$.
As shown in [23], the stability of the integration method is ensured if the eigenvalues of the amplification matrix $H(h)$ are contained in the unit circle i.e. the moduli of the eigenvalues are lower than unity.
To prove the stability of our temporal scheme let us consider the simplest case where $f_x^e = 0$ everywhere and f_x^p is a constant equals to 10. Let us also consider the case of the unconditionally stable Newmark scheme ie $\beta = 0.25$ and $\gamma = 0.5$. We will consider several values of time steps and for each of them we will plot the eigenvalues of the amplification matrix in the complex plane. For h taking its value from 0.001 to 10 by step of 0.001 we obtain the following figure :

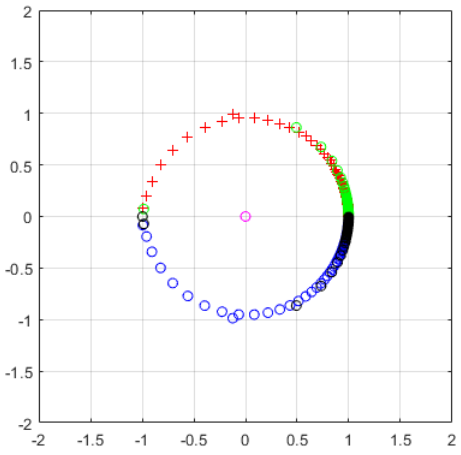

FIGURE 7 – Eigenvalues of the amplification matrix in the complex plane

As we can observe on figure 7, the eigenvalues of the amplification matrix $H(h)$ for different values of h remain in the unit circle. When h increases the eigenvalues are positioned at the left of the unit circle. For small values of h the eigenvalues are at the right. For more complex case including those where the attenuation function are not assumed constant this result holds. This result ensures that the temporal integration scheme , we developed is stable in time for the one dimensional PML. This result shows that the integration scheme derived from the equation of the PML is stable in time.
In order to evaluate the properties of a numerical scheme in terms of stability, an interesting method is to look at the spectral radius, the periodicity error and the numerical damping. The spectral radius of the method is given by the modulus of the highest eigenvalue :

$$R(A) = \max_i(|\lambda_i|) \tag{55}$$

We will express this parameter in function of $\Omega = \omega h$ where $\omega = \sqrt{\frac{k}{m}}$ and $k = \frac{ES}{L_p}$. m is the mass of the bar (in our case just an element). The asymptotic value of the spectral radius for $\omega h \to \infty$ gives an information about the stability of the method over the entire frequency domain.

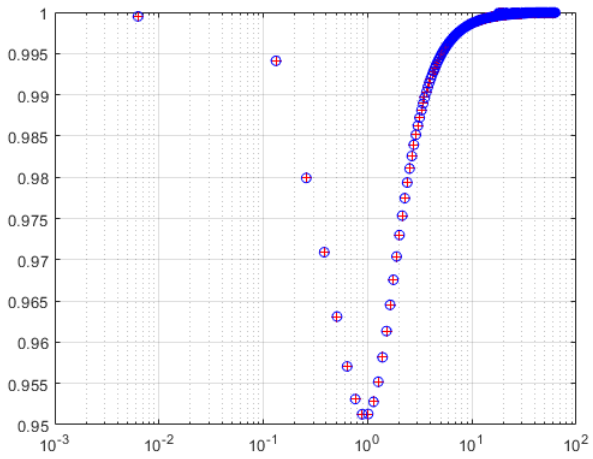

FIGURE 8 – Spectral radius in function of $h\omega$

As shown on the figure 8, the spectral radius remains under the value 1 and its asymptotic value tends to 1 as $\omega h \to \infty$. This demonstrates that the numerical scheme is stable over the entire frequency domain. Let us now focus on the periodicity error which results from the comparison between the numerical and the exact frequencies obtained for the one degree-of-freedom oscillator :

$$\frac{\Delta T}{T} = \frac{\omega h}{\phi} - 1 \qquad \text{where} \qquad \phi = tan^{-1}\left(\frac{\mathrm{Im}\,\lambda_1}{\mathrm{Re}\,\lambda_1}\right) \tag{56}$$

Therefore this is a measurement of the frequency distortion for each eigenfrequency in the model.

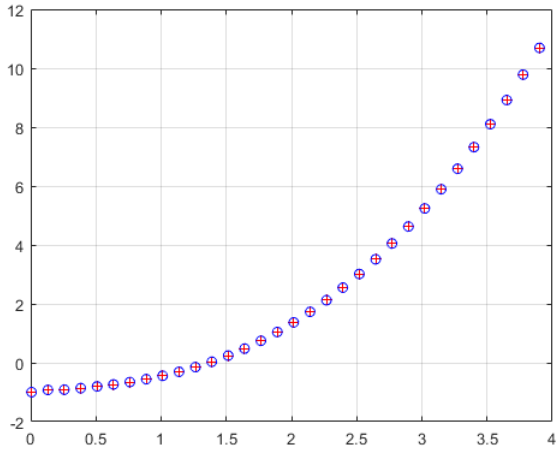

FIGURE 9 – relative periodicity error in function of $h\omega$

As observed in 9, the relative periodicity error increases with $h\omega$ looking back at the equation 56 and knowing that the modulus of each eigenvalue is smaller or equal to 1, the result obtained here about the relative periodicity error is the one expected. Since this result is difficult to interpret a more complete analysis will be done in the next report. Indeed some questions remain unanswered such as why the distortion at $h = 0$ is different than 0 or other questions about the numerical damping ratio we will

present now.
The last parameter to be investigate is the numerical damping ratio. It compare the time decay coefficient of the real part of the solution to the numerical frequency.

$$\xi = -\frac{log(|\lambda_1|)}{\phi} \tag{57}$$

It measures the percentage of critical damping introduced in the system by the integration operator. In fact it is expected to damped out the high frequencies introduced by the time integration operator.

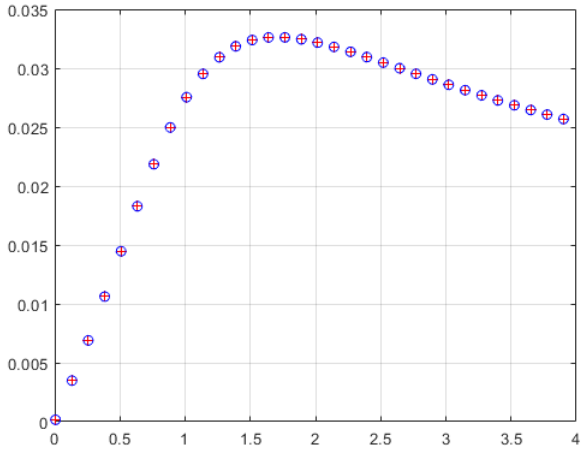

FIGURE 10 – Numerical damping ratio in function of $h\omega$

In order to compare the results obtained on the Newmark-β unconditionally stable scheme, let us make the same analysis of stability on the Newmark explicit temporal integration scheme for the PML with $\beta = 0$ and $\alpha = 0.5$ (central differences).

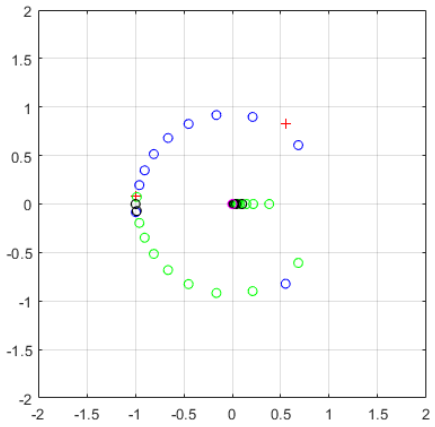

FIGURE 11 – Eigenvalues in the complex plane

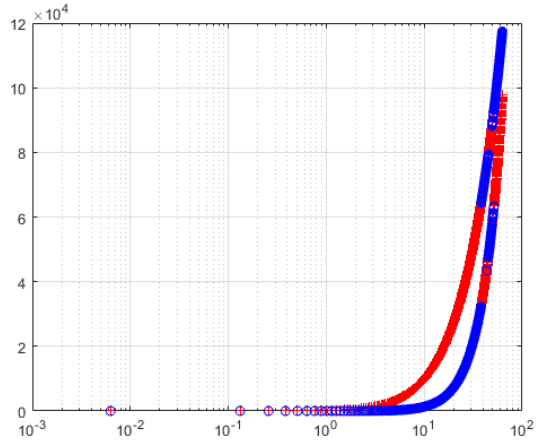

FIGURE 12 – Spectral radius in function of $h\omega$

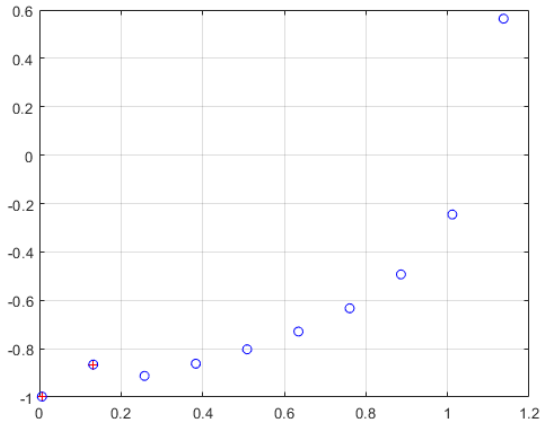

FIGURE 13 – relative periodicity error in function of $h\omega$

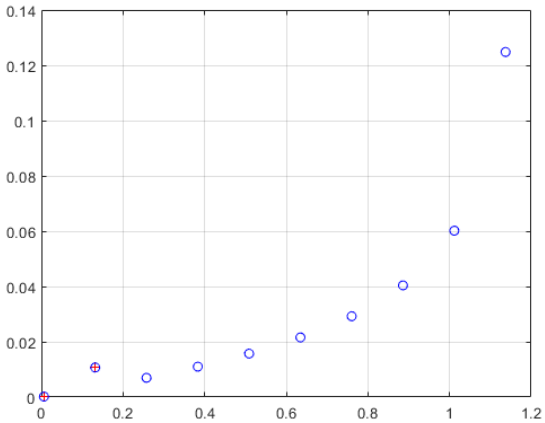

FIGURE 14 – Numerical damping ratio in function of $h\omega$

As expected for a conditionally stable scheme, passed a certain value of $h\omega$ the scheme becomes unstable. This limit of stability is evaluated $h\omega = 2$ corresponding to the CFL condition.
We can also look at the behaviour of the Newmark explicit time integrator on the physical medium. In this case the equation of motion are the same as in a classic elastodynamic problem. In the following equation the state vector q will be defined by $q^n = [\dot{u}^n, u^n]^T$. THe equation of motion at time t^n and t^{n+1} are :

$$\begin{aligned} M\ddot{u}^n &= -C\dot{u}^n - Ku^n + p^n \\ M\ddot{u}^{n+1} &= -C\dot{u}^{n+1} - Ku^{n+1} + p^{n+1} \end{aligned} \tag{58}$$

And taking into account the recurrence relationship given by the Newmark method :

$$\begin{aligned} M\dot{u}^{n+1} &= M\dot{u}^n + h(1-\gamma)\left[-C\dot{u}^n - Ku^n + p^n\right] + \gamma h\left[-C\dot{u}^{n+1} - Ku^{n+1} + p^{n+1}\right] \\ Mu^{n+1} &= Mu^n + hM\dot{u}^n + h^2(\frac{1}{2} - \beta)\left[-C\dot{u}^n - Ku^n + p^n\right] + \beta h^2\left[-C\dot{u}^{n+1} - Ku^{n+1} + p^{n+1}\right] \end{aligned} \tag{59}$$

Therefore we can define the matrix form of this recurrence :

$$q^{n+1} = A(h)q^n + g^{n+1}(h) \tag{60}$$

The component of this relation can be defined using the equations 59. We obtain :

$$A(h) = \begin{bmatrix} M + \gamma hC & \gamma hK \\ \beta h^2 C & M + \beta h^2 K \end{bmatrix}^{-1} \begin{bmatrix} (1-\gamma)hC - M & (1-\gamma)hK \\ (\frac{1}{2} - \beta)h^2 C - hM & (\frac{1}{2} - \beta)h^2 K - M \end{bmatrix} \tag{61}$$

and where

$$g^{n+1} = \begin{bmatrix} M + \gamma hC & \gamma hK \\ \beta h^2 C & M + \beta h^2 K \end{bmatrix}^{-1} \begin{bmatrix} (1-\gamma)hp^n + \gamma hp^{n+1} \\ (\frac{1}{2} - \beta)h^2 p^n + \beta h^2 p^{n+1} \end{bmatrix} \tag{62}$$

The matrix $A(h)$ is the matrix of amplification, its eigenvalues represents the normal vibration modes of the one dimensional element considered. Since the physical medium was assumed to have no damping $C = 0$. Let us now expend the solution with respect to the eigenmodes of the structure. The equations of motion can be reduced to uncoupled normal equations :

$$\ddot{\eta}^n = -\omega \eta^n + \phi^n \tag{63}$$

where ϕ^n is the participation factor at the excitation at time t^n. Thus using this system of uncoupled equations we can redifine the amplification matrix by :

$$A(h) = \begin{bmatrix} 1 & \gamma h\omega^2 \\ 0 & 1 + \beta h^2 \omega^2 \end{bmatrix}^{-1} \begin{bmatrix} 1 & -(1-\gamma)h\omega^2 \\ h & 1 - (\frac{1}{2} - \beta)h^2\omega^2 \end{bmatrix} \tag{64}$$

Using this definition of the amplification matrix, we can do the same analysis for the physical medium than the one done of the implicit Newmark scheme on the PML.

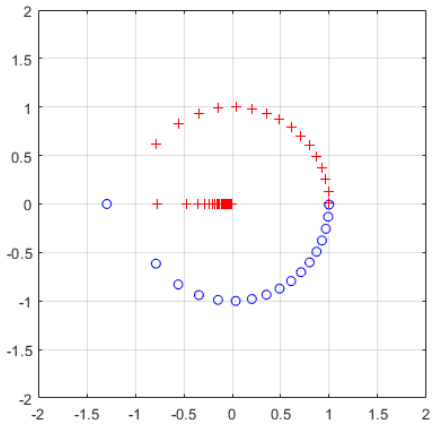

FIGURE 15 – Eigenvalues in the complex plane

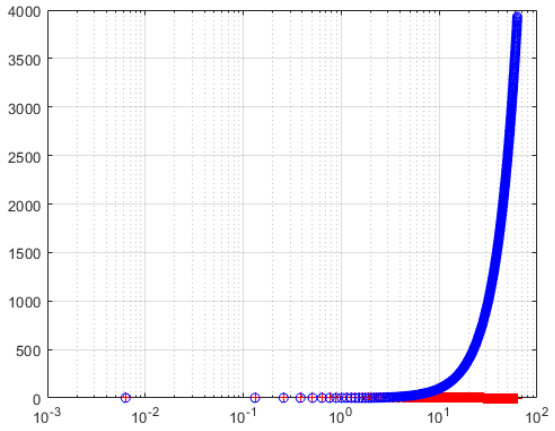

FIGURE 16 – Spectral radius in function of $h\omega$

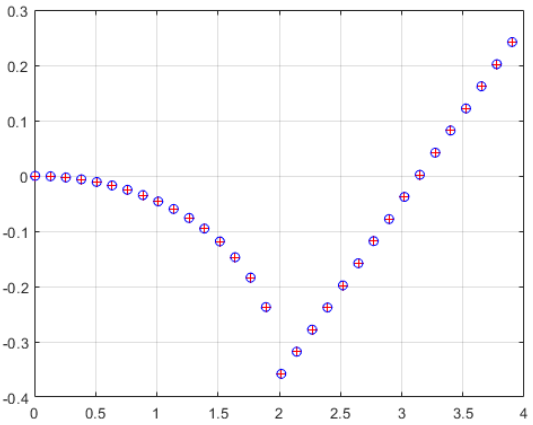

FIGURE 17 – relative periodicity error in function of $h\omega$

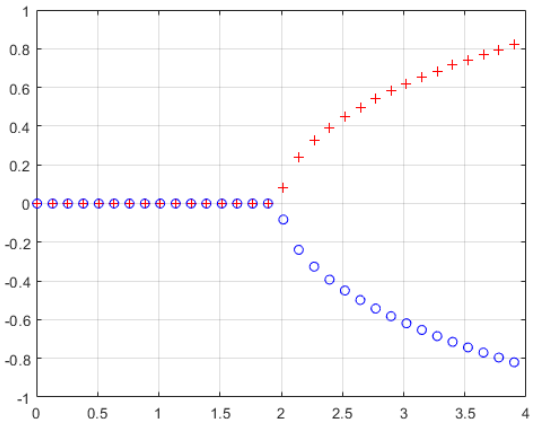

FIGURE 18 – Numerical damping ratio in function of $h\omega$

We can observe on the figure 15 that for a certain value of h the eigenvalues seems to exit the unit circle. This is the proof that at a certain point the scheme becomes unstable and amplified drastically even small perturbations. This change from stable to unstable occurs when $h\omega > 2$ as we can see on the other figures

Conclusion

The development and the analysis of the PML show two of the main aspects of the perfectly matched layers method : its power to attenuate propagating waves and but also its complexity. Indeed we have seen the full development of the equations required to construct the one dimensional PML. Starting from the simple governing equations of a linear elastodynamic problem such as the equation of motion, the constitutive equation and the strain-displacement relationship, we derived a new problem by introducing the complex coordinates and the stretching function λ. This development allows us to obtain the strong form of the PML. Going from this formulation, we were able to construct the weak form of the PML by introducing virtual displacement in order to implement these equations using the finite elements method. Using a Newmark temporal integration method, we were capable of construct an implicit scheme on the PML for wave propagation and therefore its attenuation. As we have seen the scheme presents a very accurate behavior : it attenuates completely the wave and without any reflection from the truncation interface (using a appropriate set of parameters that we highlighted in the analysis of the effects of the parameters).
The analysis of the numerical stability proves that this implicit scheme is also unconditionally stable and shows the critical value of time step h for the explicit scheme used for the propagation of the wave in the physical medium.
However certain points remains unclear in this analysis and we need to focus in detail in how to interpret correctly the results of the numerical damping and the relative periodicity error. They will give us more information about the behavior of the scheme and its stability for the PML but also for the physical medium.
In future works we will also include a complete analysis of the computational cost of this method : computational resources and time of execution. This will be a prerequisite before implementing the PML into a finite elements code (Akantu).
We will also extend this method to the two and three dimensional cases and for anisotropic medium. The same analysis of complexity, stability and computational cost will also be done in order to provide the perfectly matched layers method for the simulation of wave propagation on unbounded domains with the maximum of information and analysis.

Références

[1] Gottlieb D. Abarbanel S. A mathematical analysis of the pml method. *Journal of Computational Physics*, 134(2) :357–363, 1997.

[2] Gottlieb D. Abarbanel S. On the construction and analysis of absorbing layers in cem. *Applied Numerical Mathematics*, 27(4) :331–340, 1998.

[3] Hesthaven J.S. Abarbanel S., Gottlieb D. Long time behavior of the perfectly matched layer equations in computational electromagnetics. *Journal of Scientific Computing*, 17(1-4) :405–422, 2002.

[4] Engquist B. and Majda A. Absorbing boundary conditions for the numerical simulation of waves. *Mathematics of computation*, 31(139) :629–651, 1977.

[5] Chopra A. K. Basu U. Perfectly matched layers for time-harmonic elastodynamics of unbounded domains : theory and finite-element implementation. *Computational methods in applied mechanics and engineering*, 192 :1337–1375, 2003.

[6] Chopra A. K. Basu U. Perfectly matched layers for transient elastodynamics of unbounded domains. *International Journal For Numerical Methods in Engineering*, 59 :1039–1074, 2004.

[7] Fauqueux S. Bécache E. and Joly .P. Stability of perfectly matched layers, group velocities and anisotropic waves. *Journal of Computational Physics*, 188(2) :399–443, 2003.

[8] Tsogka C. Bécache E., Joly P. Fictitious domains, mixed finite elements and perfectly matched layers for 2-d elastic wave propagation. *Journal of Computational Acoustics*, 9(3) :1175–1201, 2001.

[9] Liu Q.H. Chew W.C. Perfectly matched layers for elastodynamics : A new absorbing boundary condition. *Journal of Computational Acoustics*, 4(4) :341–359, 1996.

[10] Weedon W.H. Chew W.C. A 3d perfectly matched medium from modified maxwell's equations with stretched coordinates. *Microwave and Optical Technology Letters*, 7(13) :599–604, 1994.

[11] Fauqueux S. Cohen G. Mixed spectral finite elements for the linear elasticity system in unbounded domains. *SIAM Journal on Scientific Computing*, 26(3) :864–884, 2005.

[12] Tsogka C. Collino F. Application of the perfectly matched absorbing layer model to the linear elastodynamic problem in anisotropic heterogeneous media. *Geophysics*, 66(1) :294–307, 2001.

[13] Giannopoulos A. Drossaert F.H. Complex frequency shifted convolution pml for fdtd modelling of elastic waves. *Wave Motion*, 44(7–8) :593–604, 2007.

[14] Giannopoulos A. Drossaert F.H. A nonsplit complex frequency-shifted pml based on recursive integration for fdtd modeling of elastic waves. *Geophysics*, 72(2) :T9–T17, 2007.

[15] Vilotte J.-P. Festa G. The newmark scheme as velocity–stress time-staggering : an efficient pml implementation for spectral element simulations of elastodynamics. *Geophysical Journal International*, 161 :789–812, 2005.

[16] Hu F.Q. On absorbing boundary conditions for linearized euler equations by a perfectly matched layer. *Journal of Computational Physics*, 129(1) :201–219, 1996.

[17] Turkel E. Harari I., Slavutin M. Analytical and numerical studies of a finite element pml for the helmholtz equation. *Journal of Computational Acoustics*, 8(1) :121–137, 2000.

[18] Broschat S.L. Hastings F.D., Schneider J.B. Application of the perfectly matched layer (pml) absorbing boundary condition to elastic wave propagation. *Journal of the Acoustical Society of America*, 14(100) :3061–3069, 1996.

[19] Bérenger J.-P. A perfectly matched layer for the absorption of electromagnetic waves. *Journal of Computational Physics*, 114(2) :185–200, 1994.

[20] Tromp J. Komatitsch D. A perfectly matched layer absorbing boundary condition for the second-order seismic wave equation. *Geophysical Journal International*, 154 :146–153, 2003.

[21] Kallivokas L.F. Kucukcoban S. Mixed perfectly-matched-layers for direct transient analysis in 2d elastic heterogeneous media. *Computational Methods in Applied Mechanics and Engineering.*, 200 :57–76, 2011.

[22] Kallivokas L.F. Kucukcoban S. A symmetric hybrid formulation for transient wave simulations in pml-truncated heterogeneous media. *Wave Motion*, 50 :57–79, 2013.

[23] Géradin M. and Rixen D. *Mechanical vibrations : Theory and applications to structural dynamics, second edition.* John Wiley and sons, 1997.

[24] Papageorgiou A.S. Meza-Fajardo K.C. A nonconvolutional, split-field, perfectly matched layer for wave propagation in isotropic and anisotropic elastic media : stability analysis. *Bulletin of the Seismological Society of America*, 98(4) :1811–1836, 2008.

[25] Bettess P. Infinite elements. *International Journal for Numerical Methods in Engineering*, 11(1) :53–64, 1977.

[26] Liu Q.H. Perfectly matched layers for elastic waves in cylindrical coordinates. *Journal of the Acoustical Society of America*, 105(4) :2075–2084, 1999.

[27] Geers T.L. Qi Q. Evaluation of the perfectly matched layer for computational acoustics. *Journal of the Acoustical Society of America*, 100(5) :3061–3069, 1996.

[28] Ungless RL. An infinite element method, masc thesis. *University of British Columbia*, 11(1) :53–64, 1973.

[29] Gedney S.D. Roden J.A. An efficient fdtd implementation of the pml with cfs in general media. *IEEE Antennas Propagat. Soc. Int. Symp.*, 3(2000) :1265–1362, 2000.

[30] Lenti L. Semblat JF and Gandomzadeh A. A simple multi-directional absorbing layer method to simulate elastic wave propagation in unbounded domains. *International journal for numerical methods in engineering*, 2010.

[31] Belytschko T. *Nonlinear finite elements for continua and structures.* Chichester : Wiley, 2013.

[32] Chew W.C. Teixeira F.L. On causality and dynamic stability of perfectly matched layers for fdtd simulations. *IEEE Trans. Microwave Theory Tech.*, 47(6) :775–785, 1999.

[33] Yefet A. Turkel E. Absorbing pml boundary layers for wave-like equations. *Applied Numerical Mathematics*, 27(4) :533–557, 1998.

[34] Basu U. Explicit finite element perfectly matched layer for transient three-dimensional elastic waves. *International Journal For Numerical Methods in Engineering*, 44 :151–176, 2008.

[35] Tang X. Wang T. Finite-difference modeling of elastic wave propagation : a nonsplitting perfectly matched layer approach. *Geophysics*, 68(5) :1749–1755, 2003.

[36] Liu Q.H. Zeng Y.Q., He J.Q. The application of the perfectly matched layer in numerical modeling of wave propagation in poroelastic media. *Geophysics*, 66(4) :1258–1266, 2001.

[37] Ballmann J. Zhang Y.-G. Two techniques for the absorption of elastic waves using an artificial transition layer. *Wave Motion*, 25(1) :15–33, 1997.